VACCINES

A respiratory syncytial virus (RSV) F protein nanoparticle vaccine focuses antibody responses to a conserved neutralization domain

Kurt A. Swanson[1]*†, Jennifer N. Rainho-Tomko[2]*, Zachary P. Williams[2]*‡, Lilibeth Lanza[2], Michael Peredelchuk[2], Michael Kishko[3], Vincent Pavot[4], Judith Alamares-Sapuay[3], Haritha Adhikarla[3]§, Sankalp Gupta[3], Sudha Chivukula[3], Scott Gallichan[5], Linong Zhang[3], Nicholas Jackson[3]||, Heesik Yoon[2], Darin Edwards[2]¶, Chih-Jen Wei[1]#, Gary J. Nabel[6]#

A stabilized form of the respiratory syncytial virus (RSV) fusion (F) protein has been explored as a vaccine to prevent viral infection because it presents several potent neutralizing epitopes. Here, we used a structure-based rational design to optimize antigen presentation and focus antibody (Ab) responses to key epitopes on the pre-fusion (pre-F) protein. This protein was fused to ferritin nanoparticles (pre-F-NP) and modified with glycans to mask nonneutralizing or poorly neutralizing epitopes to further focus the Ab response. The multimeric pre-F-NP elicited durable pre-F–specific Abs in nonhuman primates (NHPs) after >150 days and elicited potent neutralizing Ab (NAb) responses in mice and NHPs in vivo, as well as in human cells evaluated in the in vitro MIMIC system. This optimized pre-F-NP stimulated a more potent Ab response than a representative pre-F trimer, DS-Cav1. Collectively, this pre-F vaccine increased the generation of NAbs targeting the desired pre-F conformation, an attribute that facilitates the development of an effective RSV vaccine.

INTRODUCTION

Respiratory syncytial virus (RSV) is a major cause of severe respiratory disease among the high-risk populations of infants and the elderly (*1*, *2*). This susceptibility is due, in part, to waning maternal antibody (Ab) levels in infants or immune senescence in the elderly (*3*–*5*). In the case of RSV, the titer of circulating Ab specific to RSV does not diminish with age (*6*). Serious adverse events encountered in a trial of a formalin-inactivated whole virus vaccine in the 1960s included enhanced disease among vaccinees that impeded progress in the field (*7*). There is currently no licensed vaccine available against RSV (*8*, *9*).

Progress in understanding the molecular recognition of a protective monoclonal Ab to RSV fusion (F) protein has catalyzed improvements in structure-based RSV vaccine design (*8*, *10*, *11*). Attempts to develop protein subunit vaccines targeting elderly and maternal populations have been reported using the well-conserved F protein (*8*, *12*). Recent efforts using various modalities ranging from virus-like particles to post-fusion (post-F) subunit vaccines have also fallen short of providing notable protection in clinical trials (*13*, *14*).

RSV F, a trimeric protein anchored on the viral surface, mediates viral fusion. It is expressed as a single-chain precursor that is cleaved intracellularly by a furin protease (*15*). Furin cleaves the protein at two sites surrounding a 27–amino acid sequence, releasing a hydrophobic fusion peptide essential for protein function (*16*). Crystal structures have demonstrated that F exists in at least two alternative conformations: the pre-F and post-F trimer forms (*17*–*19*). Without stabilization, the F ectodomain flips spontaneously to the post-F conformation. Crystal structures of the F protein ectodomain stabilized in the pre-F conformation have been described (*20*–*22*). An early prototype of the pre-F protein, DS-Cav1 (*21*), used an engineered disulfide bond to stabilize the globular head, and a foldon trimerization motif stabilized the trimer. In animal studies, this pre-F trimer elicited a higher neutralizing titer compared with post-F antigens. In first-in-human studies, DS-Cav1 elicited neutralizing Abs (NAbs) to the pre-F surface (*23*). Studies interrogating the structure of the F protein and RSV NAbs identified the most effective epitopes, sites 0 and V, which are exposed only in the pre-F conformation (*19*, *24*, *25*).

Although disulfide stabilization used for DS-Cav1 produces a pre-F immunogen, it was reported that this antigen was not stable during long-term storage (*20*). Deletion of the furin cleavage sites prevented cleavage into the two protomer chains and permitted retention of a pre-F epitope on a single-chain F subunit without additional stabilization (*26*). A second crystal structure of a pre-F antigen using the single-chain strategy with a proline mutation to further disrupt adoption of the post-F conformation represented a next-generation antigen with increased stability relative to DS-Cav1 (*20*).

Another approach for presenting the F antigen in the pre-F conformation was described using a computationally designed nanoparticle platform (*27*). In this system, the C terminus of DS-Cav1 was fused to a self-assembling nanoparticle that displays the F antigen in a multimeric array. DS-Cav1 presented on the nanoparticle exhibited superior stability over the DS-Cav1 trimer as judged by binding to key pre-F Abs. Last, the DS-Cav1 nanoparticle elicited a higher NAb response compared with immunization with DS-Cav1 trimer. Marcandalli *et al.* (*27*) suggested that one potential explanation for the improved quality of response was that more potent neutralizing

[1]Sanofi, 270 Albany, Cambridge, MA 02139, USA. [2]Sanofi Pasteur VaxDesign, 2501 Discovery Drive, Suite 300, Orlando, FL 32826, USA. [3]Sanofi Pasteur, 38 Sidney Street, Cambridge, MA 02139, USA. [4]Sanofi Pasteur, 1541 Avenue Marcel Mérieux, Marcy l'Etoile, France. [5]Sanofi Pasteur, 95 Willowdale Blvd, Toronto, Ontario, Canada. [6]Sanofi, 640 Memorial Drive, Cambridge, MA 02139, USA.
*These authors contributed equally to this work.
†Present address: Ring Therapeutics, Cambridge, MA 02139, USA.
‡Present address: AbbVie Inc., North Chicago, IL 60064, USA.
§Present address: Sanofi, 1 Discovery Drive, Swiftwater, PA 18730, USA.
||Present address: CEPI, London, UK.
¶Present address: Moderna Inc., Cambridge, MA 02139, USA.
#Corresponding author. Email: gary.nabel@sanofi.com (G.J.N.); chih-jen.wei@sanofi.com (C.-J.W.)

epitopes, such as site 0, were more exposed in the nanoparticle format relative to the less potent epitopes near the stalk, which were partially occluded by the nanoparticle display. Ab-dependent enhancement (ADE) represents a potential mechanism that might increase the severity of RSV infection or enhance immunopathology (*28*, *29*). However, there has been no clinically proven evidence for ADE in seropositive elderly populations, and there has been a recent study describing a lack of association between in vitro–demonstrated ADE and disease severity in children (*30*). Given the potential impact of ADE in vaccine recipients if ADE occurs in vivo in RSV, it is reasonable in the development of an RSV vaccine to consider both the serostatus of the population and the quality of response by assessment of neutralizing versus binding Ab titers.

Here, we describe a multimeric RSV F immunogen that fuses pre-F to a self-assembling ferritin nanoparticle previously shown to enhance the immunogenicity of influenza and Epstein-Barr virus (EBV) vaccines (*31*–*35*). Ab binding and negative-staining electron microscopy (EM) confirms that the particle is homogeneous and displays the expected eight pre-F moieties. The F moieties are oriented so that the most potent NAb epitopes are exposed and the lesser neutralizing epitopes are oriented toward the stalk. We further focused the immune response by introducing glycosylation sites that reduced Ab titers to nonneutralizing or poorly neutralizing epitopes, improving the quality of response as measured by the increased neutralizing to binding Ab ratio. The pre-F-NP immunogen was also fused to a bacterial ferritin nanoparticle used safely in human trials, expressed as a single self-assembling protomer, with yields in stable cell lines that are suitable for large-scale manufacturing. Pre-F-NP elicited NAbs in mouse and nonhuman primate (NHP) models. Analysis using the biomimetic Modular Immune In vitro Construct (MIMIC) system (*36*) evaluated the potential of pre-F-NP to boost a response from human individuals, suggesting that these modifications might contribute to improved RSV immunogenicity clinically.

RESULTS

Design, screening, and in vitro assembly of pre-F nanoparticles

Prototype pre-F-NPs were developed by introducing the ferritin sequence from *Helicobacter pylori* at the C terminus of DS-Cav1 (DS-Cav1-NP) (*37*). The nanoparticle is composed of 24 subunits of ferritin with an N-terminal threefold axis of symmetry that allowed the F protomers to form eight pre-F trimeric spikes. DS-Cav1-NP formed particles that bound pre-F-Abs; however, the yields (0.87 mg/liter) measured by pre-F–specific AM14 Ab were suboptimal. AM14 is a monoclonal Ab that recognizes a quaternary epitope specific to pre-F and therefore confirms trimer formation (*38*). To improve yield, we deleted the furin cleavage and p27 regions to generate a stabilized single-chain F and added a bullfrog ferritin linker previously used for an EBV ferritin nanoparticle (*35*). This single-chain (sc) particle retained the engineered disulfide bond and cavity-filling mutations of DS-Cav1 (sc-pre-F-NP) and improved expression about

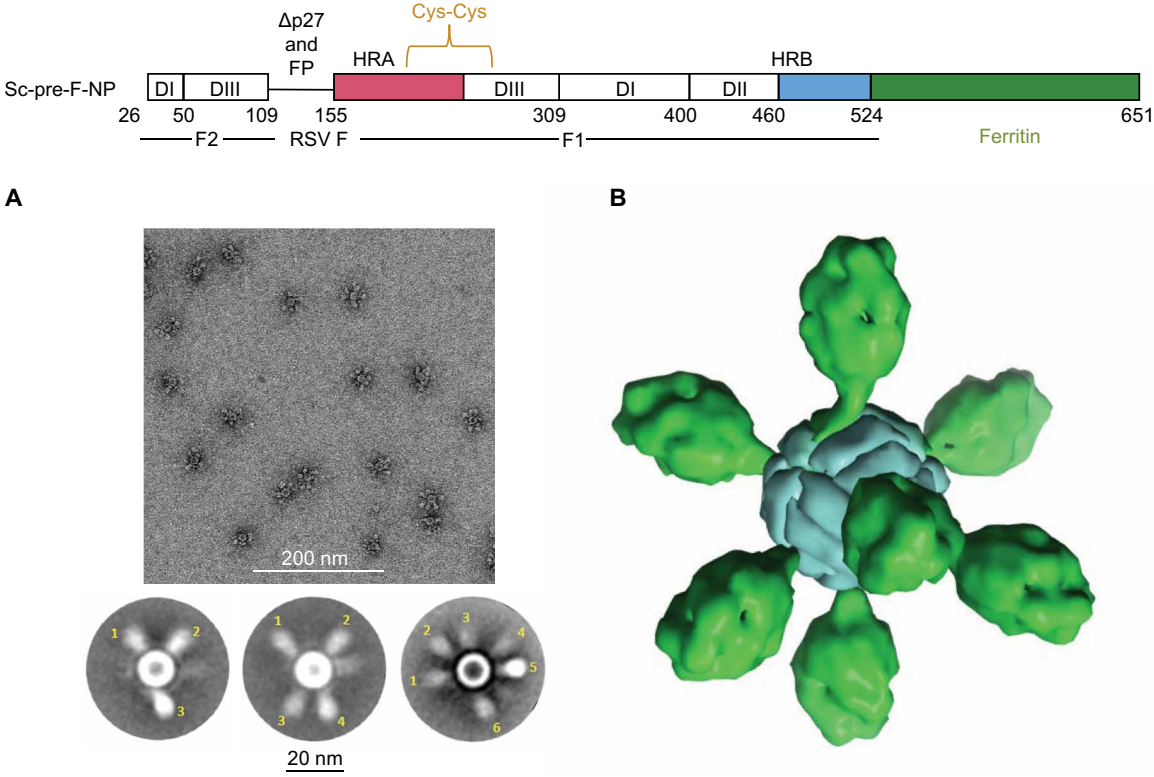

Fig. 1. Sc-pre-F-NP structure. Linear diagram of sc-pre-F-NP antigen. Residue numbers corresponding to the N terminus of each segment are indicated below the segment. Domains 1 to 3 are indicated (DI, DII, and DIII), heptad repeat region A (HRA) is in red, and heptad repeat region B (HRB) is in blue. Δp27 and FP (fusion peptide) indicates where the p27 and FP have been deleted and replaced with the single-chain linker. A yellow bracket labeled Cys-Cys shows the engineered disulfide bond. The green segment indicates the ferritin particle moiety, as labeled below. (**A**) Negative-stained EM image of sc-pre-F-NP showing that the molecule forms homogeneous nanoparticles. (**B**) 2D EM class averages of pre-F-NP show the expected symmetry of eight spherical F spikes consistent with the pre-F nanoparticle structural model.

twofold (1.35 mg/liter). Sc-pre-F-NP formed homogeneous nanoparticles with the expected eight F spikes predicted by structural modeling, as demonstrated by negative-staining EM and two-dimensional (2D) class averaging (Fig. 1, A and B).

To enhance expression of sc-pre-F-NP further, the cysteine mutations of the DS-Cav1–engineered disulfide were mutated to their native serine residues. In addition, we mutated residue I217, which caps the N terminus of a central helix that forms interprotomer contacts in the center of the pre-F globular head, to proline (Fig. 2A). This mutation was intended to improve helical stability of this central helix, and the new particle (pre-F-NPΔglyc) increased expression about twofold (2.8 mg/liter). Last, we added glycan sites on the pre-F surface to regions of the trimer surface that would not occlude known neutralizing epitopes (Fig. 2B). After screening nearly 100 variants for expression and ability to bind NAbs and particle formation by negative-staining EM, we identified a lead pre-F-NP vaccine candidate that increased expression more than fivefold relative to the initial DS-Cav1-NP prototype (4.7 mg/liter).

Multimeric presentation and blocking post-F sites with glycans enhances pre-F-NP immunogenicity in mice and NHPs

Naïve mice were immunized with three injections of either pre-F-NP or post-F trimer mixed with the squalene-based adjuvant AF03 (*39*). Pre-F-NP elicited a DS-Cav1–binding (pre-F–binding) Ab response (titer ~10^2) and elicited about 100-fold increase in NAb titer relative to post-F (Fig. 3, A and B). In NHPs, two injections of pre-F-NP adjuvanted with AF03 elicited pre-F–binding Ab titers of ~10^5 and NAb titers of ~10^3 (Fig. 3, C and D). By comparison, unadjuvanted pre-F-NP elicited pre-F–binding Ab titers of ~10^3 and three of four NHPs did not have detectable neutralizing titers (Fig. 3, C and D). Furthermore, pre-F–binding Ab titers were observed at >10^4 for more than 150 days after second immunization in NHPs when given with AF03, relative to ~10^3 without adjuvant (fig. S1).

Glycosylation sites were designed to increase expression and avoid known neutralizing epitopes of pre-F (Fig. 2B). Specifically, glycans were added in a region of F between the major palivizumab neutralization epitope and the viral membrane stalk, which remains relatively unchanged between the pre-F and post-F structures and lacks known neutralizing epitopes.

We compared the immunogenicity of pre-F-NP with pre-F-NP that lacked these glycans (pre-F-NPΔglyc). Mice were immunized with either pre-F-NP or pre-F-NPΔglyc, and their Ab responses were characterized (Fig. 4). NAb titers elicited by the two antigens were not statistically different (Fig. 4A). In contrast, post-F–binding Ab titers elicited by pre-F-NP were significantly lower than Ab titers elicited by pre-F-NPΔglyc (Fig. 4B). Introduction of these glycans therefore reduced the generation of Abs to the nonneutralizing or poorly neutralizing epitopes without compromising RSV neutralization, thus stimulating a more focused NAb response (Fig. 4C). Similarly, in NHPs, pre-F-NP elicited ~10-fold lower post-F–binding Ab titers (~10^3) relative to pre-F–binding titers (fig. S1, A and B). Last, competition enzyme-linked immunosorbent assay (ELISA) with pre-F–specific Ab D25 confirmed the specificity of the pre-F response in NHPs (fig. S1C).

Pre-F-NP elicits a more potent NAb response than DS-Cav1

We generated stable cell lines using our Chinese hamster ovary (CHO) cell line for vaccine manufacturing (see Materials and Methods). Pre-F-NP yields from production cell lines express homogeneous material between ~150 and 300 mg/liter using a manufacturing compatible purification (fig. S2A). The CHO-derived pre-F-NP bound to NAbs with affinities similar to DS-Cav1 (fig. S2B). To test the immunogenicity of the CHO-derived pre-F-NP relative to a comparator that is being evaluated in the clinic, pre-F trimer (DS-Cav1) (*23*), naïve mice were immunized with either pre-F-NP or pre-F mixed with AF03 (Fig. 5 and fig. S3B) or without adjuvant (fig. S3A). Each group of eight mice was given two immunizations of an antigen dose (0.03, 0.1, 0.3, 1, 3, 9, or 27 μg), and the NAb titer was measured. When formulated with AF03, pre-F-NP elicited a higher neutralizing titer than DS-Cav1 at higher doses (3, 9, and 27 μg) after the first immunization (fig. S3B). After the second immunization with AF03, pre-F-NP elicited a higher neutralizing titer at lower doses (0.03, 0.1, 0.3, 1, 3, and 9 μg), whereas the DS-Cav1 response was not statistically different from pre-F-NP at the 27-μg dose (Fig. 5). After two immunizations without AF03, pre-F-NP elicited a higher neutralizing

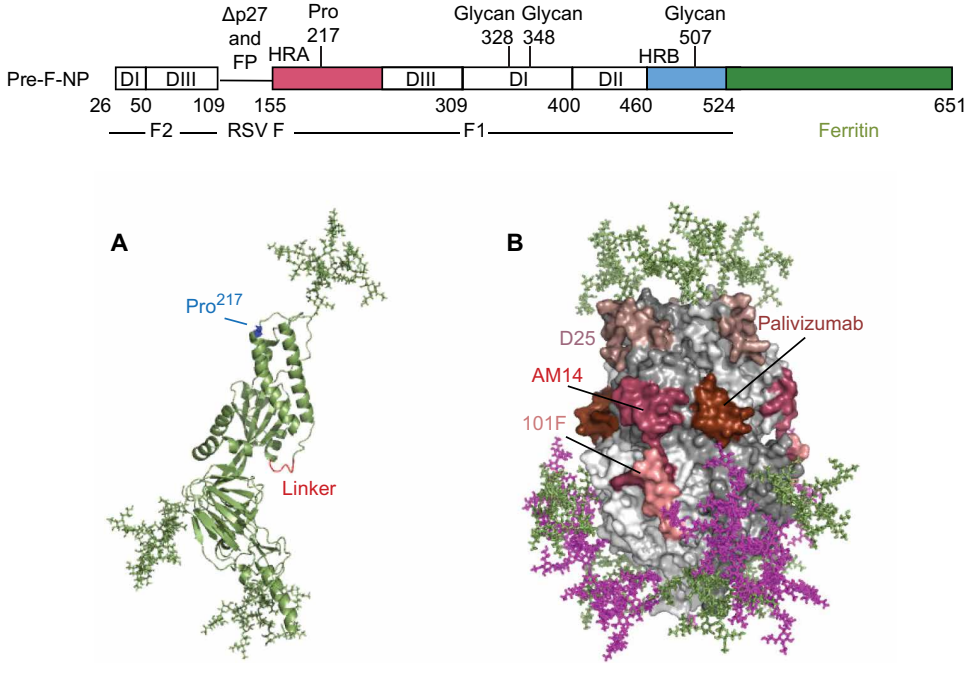

Fig. 2. Glycans block nonneutralizing epitopes on pre-F-NP. Linear diagram of pre-F-NP labeled and colored as in Fig. 1. The engineered proline residue capping the central helix, as well as the sites for the three engineered glycan sites, are indicated above. (**A**) Structural model of the single-chain F protomer showing the engineered proline in blue and single-chain linker buried in the F head in red. The three native glycans are shown in green. (**B**) Modeled structure of the single-chain F trimer spike, with native glycans colored in green and three engineered glycan sites shown in magenta. Known neutralizing epitopes are colored and labeled for reference.

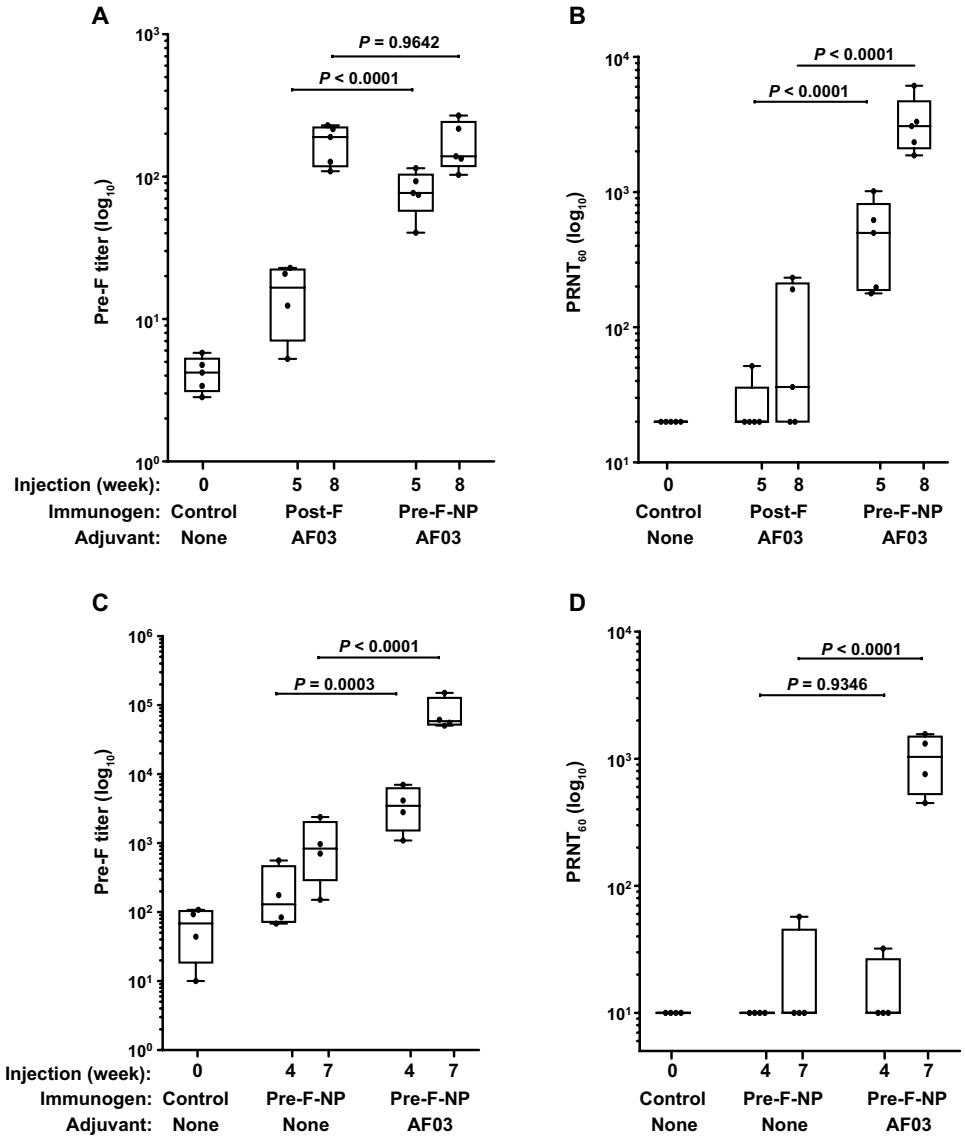

Fig. 3. NAb responses to pre-F-NP in mice and NHPs. (**A**) Pre-F–binding Ab titers after immunization with pre-F-NP or post-F with adjuvant in mice measured using Octet. In all panels, immunogens, injection number, and adjuvant use are indicated below the graph. (**B**) NAb titers induced by pre-F-NP or post-F with adjuvant in mice represented as $PRNT_{60}$. (**C**) Pre-F–binding Ab titers after immunization with pre-F-NP with or without adjuvant in NHPs measured by ELISA. (**D**) NAb titers induced by pre-F-NP in NHPs with or without adjuvant are represented as $PRNT_{60}$. Each mouse group represents five mice, and each NHP group represents four NHPs.

response than DS-Cav1 at higher doses (1, 3, 9, and 27 μg) (fig. S3A). The fold increase in NAb titer response and the statistical differences at the different doses are provided (fig. S3C).

Pre-F-NP induced more potent Ab responses compared with other subunit F vaccine candidates in the MIMIC system

We used the human in vitro platform known as MIMIC (*36*) to evaluate responses to pre-F-NP. The MIMIC platform incorporates memory B cells to investigate naïve and recall immune responses. Antigen exposure in the MIMIC system with pre-F-NP, pre-F trimer, and post-F trimer antigens stimulated higher pre-F–binding Ab titers compared with unstimulated controls (Fig. 6A). Pre-F-NP stimulated statistically higher levels of pre-F–binding Ab titers (Fig. 6A) and neutralization titers (Fig. 6B) compared with molar equivalent doses of post-F. Pre-F-NP increased the average level of pre-F–binding Ab titers by about 15-fold relative to unstimulated controls, whereas stimulation with pre-F increased pre-F–binding titers by ~6-fold. The mean neutralization titer also substantially increased after exposure to pre-F-NP (18.9 IU/ml) compared with pre-F (10.9 IU/ml) and post-F (9.8 IU/ml). In addition, pre-F-NP stimulated higher Ab titers specific for pre-F than pre-F or post-F trimer (Fig. 6C).

Pre-immune status to RSV affects Ab response to RSV, and pre-F-NP improves Ab responses in human recall response

The magnitude of the Ab response to F subunit vaccine candidates was evaluated on the basis of the serologic status of the human individuals investigated in the MIMIC system (fig. S4). Post-F, pre-F, and pre-F-NP induced a higher fold increase in pre-F–binding titers in individuals with high baseline titers (9.6-, 9.0-, and 22.32-fold increase, respectively) than low baseline titer individuals (1.3-, 2.58-, and 15.5-fold, respectively; Fig. 7A). A similar trend was observed in the subset of individuals tested for increased NAb titers between higher baseline (64, 64, and 91% responders) and low baseline pre-F–binding titer individuals (25, 50, and 67% responders; Fig. 7B).

Post-F showed a significant fold increase in pre-F binding between the low and high baseline individuals (1.35-fold versus 9.6-fold increase; $P = 0.0096$). Regardless of serologic status, pre-F-NP induced a significantly higher fold change in pre-F–binding response relative to pre-F and post-F. Pre-F elicited a significantly higher fold increase in pre-F–binding titers ($P = 0.0007$; Fig. 7A) and NAb titer ($P = 0.0449$; Fig. 7B) than post-F in individuals with low baseline titers. In individuals with high baseline titers, the percentage of nonresponders (individuals with NAb titers less than $1{:}2^5$) were the same between pre-F and post-F (Fig. 7B).

DISCUSSION

RSV is a major cause of severe respiratory diseases in infants and the elderly. Despite decades of intensive effort, an effective vaccine to protect these vulnerable populations remains a major unmet medical need (*1*, *2*). In past and ongoing trials, the envelope F protein has been a major target for RSV vaccine development because of its key role in the fusion event and its highly conserved nature among strains.

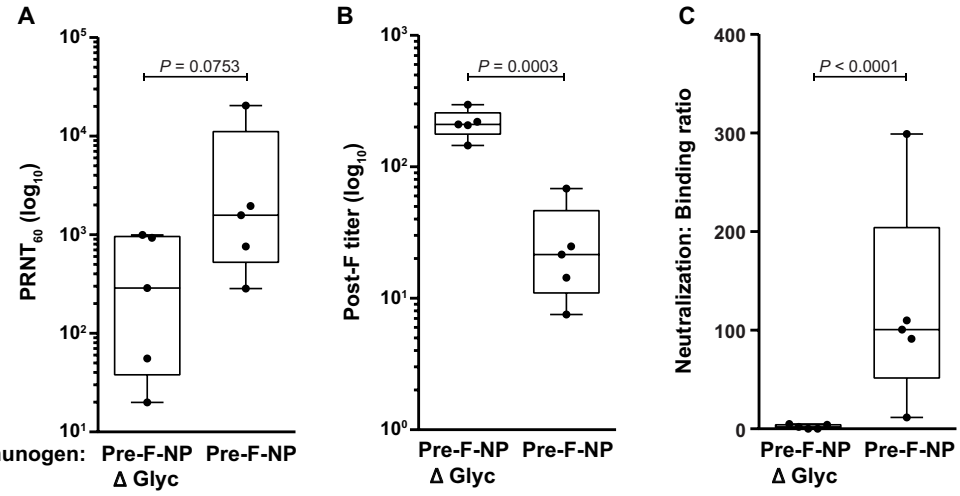

Fig. 4. Blocking nonfunctional epitopes with glycans on pre-F-NP focuses Ab responses toward pre-F epitopes in mice. (**A**) NAb titers induced by immunization with pre-F-NP or pre-F-NPΔglyc in mice represented as $PRNT_{60}$. In all panels, response is after three injections with adjuvant. (**B**) Post-F–binding Ab titers elicited by immunization with pre-F-NP or pre-F-NPΔglyc. (**C**) Ratio of RSV NAb to post-F–binding Ab titer elicited by immunization with pre-F-NP or pre-F-NPΔglyc. Each group represents five mice.

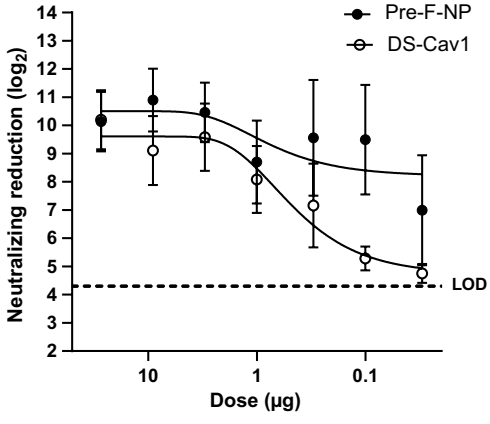

Fig. 5. NAb responses to pre-F and pre-F-NP in mice is dependent on immunogen dose. NAb titers induced by two immunizations with pre-F-NP or pre-F with adjuvant in mice represented as $PRNT_{60}$. Immunogen dose is plotted on the *x* axis with limit of detection (LOD) as illustrated. Each point represents a geometric mean of eight mice per group. Fold differences in geometric mean titers for each dose and statistical analysis are provided in fig. S3C.

After numerous failures of post-F vaccine candidates, most current RSV vaccine programs are focused on pre-F candidates, and many approaches to stabilizing the conformation of the antigen are under evaluation. Our pre-F-NP vaccine candidate used ferritin nanoparticle technology to display eight pre-F moieties and harbored engineered glycosylation sites to mask nonneutralizing epitopes on the protein surface. This design resulted in elicitation of a NAb response biased toward pre-F Abs relative to post-F in both naïve mice and NHP models.

As with other pre-F antigens, pre-F-NP elicited a superior NAb response in naïve mice than Pre-F (DS-Cav1). This distinction was greater when the antigens were administered with the squalene-based adjuvant AF03 in both mice and NHP. The addition of novel glycosylation sites allowed pre-F-NP to elicit an improved NAb/binding Ab ratio. This immunofocusing may be of importance given current hypotheses suggesting that nonneutralizing or poorly neutralizing Abs may contribute to Ab disease enhancement, particularly in populations with lower RSV F baseline titers. Our glycan additions have further biased the response toward pre-F Abs relative to post-F Abs in both naïve mice and NHP models. However, naïve animal models have previously overestimated the efficacy of RSV antigens, particularly in the case of post-F antigens that protect well in naïve animal challenge models but failed to reach efficacy in the clinic.

Immunization with post-F antigens in naïve animals has been shown to provide a neutralizing response, albeit weaker than pre-F (*23*). In our mouse study, three immunizations with a low dose of post-F (0.1 μg) did provide a detectable neutralizing response (Fig. 3B) and a relatively high pre-F–binding titer given the shared epitopes between the conformations (Fig. 3A). As expected, pre-F-NP elicited a significantly higher NAb titer response, but the binding titers appeared to reach a "ceiling" in the assay. However, it is possible that the relative pre-F–binding titer elicited by pre-F-NP is reduced by the glycans added to the nonneutralizing or poorly neutralizing epitopes shared between the pre- and post-F conformations.

Because humans are exposed to RSV infection many times throughout life, circulating and tissue-resident memory pools and Abs against RSV are present. As with humoral response, human T cell responses to the RSV virus and to RSV vaccine candidates are largely dependent upon immune memory. The MIMIC system incorporates the immune history of exposure to infectious agents, including RSV (*36*, *40*). The MIMIC system has been demonstrated to reproducibly generate predictive innate and adaptive immune responses in a number of studies with published clinical correlation (*41*–*43*). Specifically, we have established the ability of this module to display reduced Ab production and T cell activation upon in vitro influenza vaccination of cells from elderly adults. In the MIMIC system, we observe similar reduction in strain-specific immunoglobulin G (IgG) production to seasonal trivalent influenza vaccine in the elderly when compared with adults as compared with ex vivo analysis completed on clinical samples. The MIMIC system may therefore allow us to incorporate considerations of RSV immune history and age-dependent responses that may better predict how the pre-F-NP vaccine candidate will compare with other F antigens in the clinical setting.

Immune history has been widely studied for its effect on protection and/or promotion of disease progression and effectiveness of vaccines (*44*–*46*). Older adults with highly neutralizing circulating Abs show a decreased risk of developing symptomatic RSV infection than individuals with lower preexisting neutralizing sera titers (*47*). Considerable debate surrounds whether age alone is a risk factor for severe morbidity during RSV infection or whether this is only the case for the "frail" elderly who have concurrent conditions, which

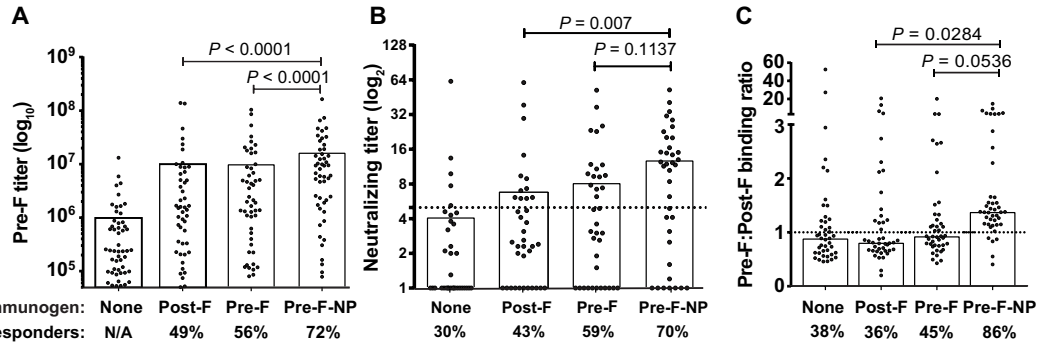

Fig. 6. Pre-F-NP elicits pre-F–directed NAbs in the MIMIC system. (**A**) Pre-F–binding titers were measured after stimulating cells with post-F, pre-F, or pre-F-NP. In each panel, immunogen used for stimulation is indicated below the graph. Each dot represents a response from individual donor, the bar indicates the geometric mean, and the percentage of individual donors who responded to stimulation is indicated. For pre-F–binding titer, a responder is considered an individual donor whose titer rose at least fivefold after stimulation. (**B**) NAb titers were measured after stimulating cells as above. The titer is given as 50% reduction in neutralizing titer, and a responder is considered an individual whose titer is at least 2^5, as indicated by the dotted line. (**C**) Measured ratios between pre-F– and post-F–binding Ab titers. A responder is considered an individual whose pre-F:post-F binding ratio is greater than 1, as indicated by the dotted line. For comparison, the untreated control is labeled as none.

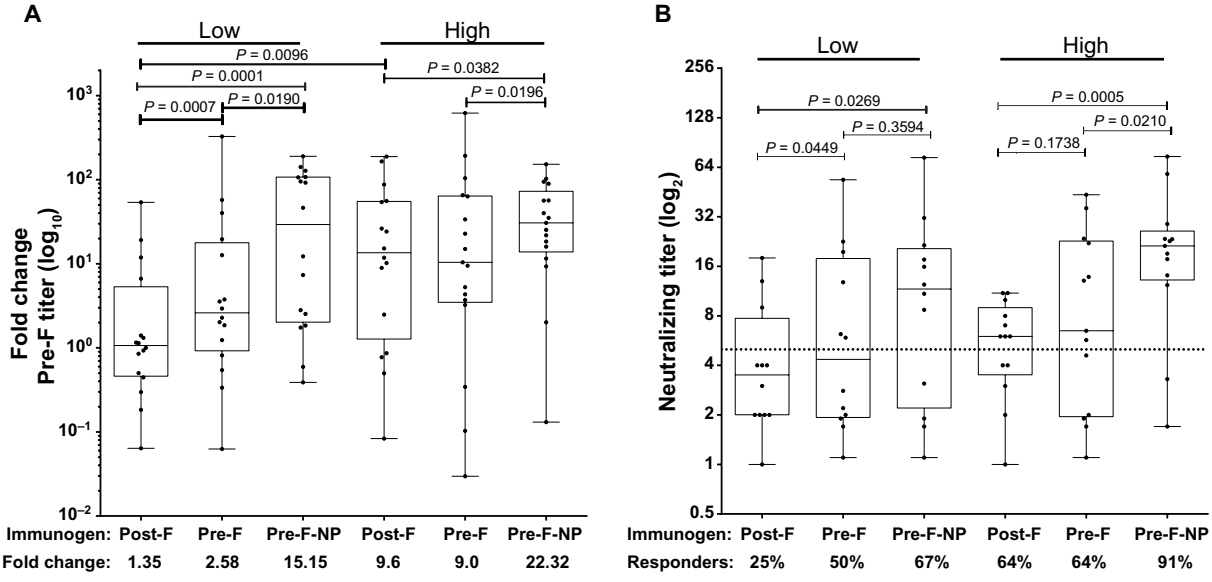

Fig. 7. Preexisting Ab titer in human individuals is strongly correlated with the magnitude of the RSV immune response in MIMIC system. (**A**) Rise in pre-F titers is shown on the basis of serologic status for 16 donors with the lowest and highest preexisting pre-F Ab titers after stimulation with post-F, pre-F, or pre-F-NP antigens. Data are presented as fold change of pre-F titer over unstimulated baseline titer. Each dot represents a response from an individual donor. Below the graph, the geometric mean fold change in titer after stimulation is shown for each immunogen. (**B**) Rise in NAb titers is shown on the basis of serologic status for 13 donors with the lowest and highest preexisting pre-F Ab titers after stimulation with F antigens. Each dot represents a response from an individual donor. The titer is given as 50% reduction in neutralizing titer, and a responder is considered an individual whose titer is at least 2^5, as indicated by the dotted line.

often coincide with senescence such as chronic obstructive pulmonary disease (*48*). When we interrogated the individual pre-F–binding responses, neutralizing responses, or T cell responses based on age, we were not able to find statistical differences (fig. S5). It is noteworthy that all the elderly individuals who provided samples for these studies were in relatively good health as a result of the selection criteria for the apheresis blood collection process, and so this analysis may not capture some age-dependent correlates of severe RSV illness in a clinical setting.

The variation observed in the human recall response can make it challenging to make meaningful observations. However, by considering the baseline pre-F–binding titer of the individuals, trends in the response can be observed (fig. S4). Although responses to each antigen trended higher for individuals with higher baseline titers, only the sevenfold increase in pre-F–binding titer between low and high baseline titer individuals elicited by post-F reached significance ($P = 0.0096$). This observation may suggest that post-F antigens can elicit a reasonable immune response in individuals with high baseline pre-F–binding titers but fail to recover protective immunity in individuals whose titers have waned. For each antigen tested, many individuals' recall responses failed to generate appreciable neutralizing titers (below the $1{:}2^5$ NAb titer) despite significant increases in

binding responses. These individuals may benefit the most from an adjuvanted immunization. The distinction between pre-F and pre-F-NP NAb titers (50 and 67% responders, respectively) failed to reach significance in the low baseline individuals, which may be due, in part, to the limited number of donors for whom NAb titers could be measured (13 versus 16 donors per group used in the F-binding comparisons) and the fact that the neutralizing assay is less sensitive. However, the trend is consistent with the statistically significant pre-F–binding responses (2.58- and 15.15-fold increase, respectively).

If the optimal target population for an RSV vaccine is not solely related to age but rather those elderly whose RSV-specific Ab titers have waned, an optimal vaccine should be targeted toward boosting the right quality of response in that specific "at-risk" population. It is interesting to note that post-F antigen elicits significantly higher fold increase in pre-F–binding Ab titers in individuals with high baseline titers than low baseline titers. It is possible that the lack of clinical efficacy observed for post-F antigens is correlated to an individual's serostatus such that post-F antigens may protect a portion of the population, but in individuals with low baseline titers, it may not protect but rather enhance RSV infection by boosting ADE-associated Abs without the accompanying NAb response. For this reason, we plan to compare the Ab responses elicited by this pre-F antigen with post-F or other pre-F antigens lacking the glycan sites in the clinical setting. Because the multimeric pre-F antigen elicits a higher neutralizing response while also improving the quality of the response, particularly in those individuals with weak preimmunity, it may serve as a vaccine well suited for the at-risk elderly population.

MATERIALS AND METHODS

Study design

The goal of this study was to evaluate immune responses to an RSV pre-F nanoparticle vaccine. Pre-F nanoparticles were produced and characterized biophysically and biochemically to confirm structural integrity of the antigen. A combination of in vitro (MIMIC) and in vivo (mouse and NHP) studies was carried out to evaluate immunogenicity. Manufacturability of this vaccine was also demonstrated in a good manufacturing practice (GMP)–compatible CHO cell line.

Antigen expression and purification from transient transfection

DNA for RSV F constructs with the described mutations was synthesized and cloned into a mammalian expression vector by GenScript. Pre-F (DS-Cav1), post-F, and RSV F Abs were generated similarly to the protocols previously published (*21*, *49*). For transient transfection material used in initial screening studies, RSV F nanoparticles were transfected into 293EXPI cells and harvested from the conditioned media after 4 days. RSV F nanoparticles were purified by an anionic exchange purification using HiTrap Q columns (GE Healthcare) with tris buffer (pH 8.5) mobile phase eluting with increasing sodium chloride concentration, followed by size exclusion purification using a Superose 6 prep grade column (GE Healthcare) and tris-buffered saline mobile phase using conventional chromatography methods. All antigens were stored at −80°C before use.

RSV F nanoparticle sequences for transient transfection

DS-Cav1-NP. mellilkanaittiltavtfcfasgqniteefyqstcsavskgylsalrtgwytsvitielsnikenkcngtdakvklikqeldkyknavtelqllmqstpatnnrarrelprfmnytlnnakktnvtlskkrkrrflgfllgvgsaiasgvavckvlhlegevnkiksallstnkavvslsngvsvltfkvldlknyidkqllpilnkqscsisnietviefqqknnrlleitrefsvnagvttpvstymltnsellslindmpitndqkklmsnnvqivrqqsysimciikeevlayvvqlplygvidtpcwklhtsplcttntkegsnicltrtdrgwycdnagsvsffpqaetckvqsnrvfcdtmnsltlpsevnlcnvdifnpkydckimtsktdvsssvitslgaivscygktkctasnknrgiiktfsngcdyvsnkgvdtvsvgntlyyvnkqegkslyvkgepiinfydplvfpsdefdasisqvnekinqslafirksdellsggssgssggsdiikllneqvnkemqssnlymsmsswcythsldgaglflfdhaaeeyehakkliiflnennvpvqltsisapehkfegltqifqkayeheqhisesinnivdhaikskdhatfnflqwyvaeqheeevlfkdildkielignenhglyladqyvkgiaksrksgs*

Sc-pre-F-NP. mellilkanaittiltavtfcfasgqniteefyqstcsavskgylsalrtgwytsvitielsnikenkcngtdakvklikqeldkyknavtelqllmgsgnvglggaiasgvavckvlhlegevnkiksallstnkavvslsngvsvltfkvldlknyidkqllpilnkqscsisnietviefqqknnrlleitrefsvnagvttpvstymltnsellslindmpitndqkklmsnnvqivrqqsysimciikeevlayvvqlplygvidtpcwklhtsplcttntkegsnicltrtdrgwycdnagsvsffpqaetckvqsnrvfcdtmnsrtlpsevnlcnvdifnpkydckimtsktdvsssvitslgaivscygktkctasnknrgiiktfsngcdyvsnkgvdtvsvgntlyyvnkqegkslyvkgepiinfydplvfpsdefdasisqvnekinqslafirksdellsggssgssggsdiikllneqvnkemqssnlymsmsswcythsldgaglflfdhaaeeyehakkliiflnennvpvqltsisapehkfegltqifqkayeheqhisesinnivdhaikckdhatfnflqwyvaeqheeevlfkdildkielignenhglyladqyvkgiaksrksgs*

Pre-F-NPΔglyc. mellilkanaittiltavtfcfasgqniteefyqstcsavskgylsalrtgwytsvitielsnikenkcngtdakvklikqeldkyknavtelqllmgsgnvglggaiasgvavskvlhlegevnkiksallstnkavvslsngvsvltfkvldlknyidkqllpilnkqscsisnpetviefqqknnrlleitrefsvnagvttpvstymltnsellslindmpitndqkklmsnnvqivrqqsysimsiikeevlayvvqlplygvidtpcwklhtsplcttntkegsnicltrtdrgwycdnagsvsffpqaetckvqsnrvfcdtmnsrtlpsevnlcnvdifnpkydckimtsktdvsssvitslgaivscygktkctasnknrgiiktfsngcdyvsnkgvdtvsvgntlyyvnkqegkslyvkgepiinfydplvfpsdefdasisqvnekinqslafirksdellsgsgsesqvrqqfskdiekllneqvnkemqssnlymsmsswsythsldgaglflfdhaaeeyehakkliiflnennvpvqltsisapehcfegltqifqkayeheqhisesinnivdhaikskdhatfnflqwyvaeqheeevlfkdildkielignenhglyladqyvkgiaksrks*

Pre-F-NP. mellilkanaittiltavtfcfasgqniteefyqstcsavskgylsalrtgwytsvitielsnikenkcngtdakvklikqeldkyknavtelqllmgsgnvglggaiasgvavskvlhlegevnkiksallstnkavvslsngvsvltfkvldlknyidkqllpilnkqscsisnpetviefqqknnrlleitrefsvnagvttpvstymltnsellslindmpitndqkklmsnnvqivrqqsysimsiikeevlayvvqlplygvidtpcwklhtsplcttntkngsnicltrtdrgwycdnagnvsffpqaetckvqsnrvfcdtmnsrtlpsevnlcnvdifnpkydckimtsktdvsssvitslgaivscygktkctasnknrgiiktfsngcdyvsnkgvdtvsvgntlyyvnkqegkslyvkgepiinfydplvfpsdefdasisqvnekinqslafinksdellsgsgsesqvrqqfskdiekllneqvnkemqssnlymsmsswsythsldgaglflfdhaaeeyehakkliiflnennvpvqltsisapehcfegltqifqkayeheqhisesinnivdhaikskdhatfnflqwyvaeqheeevlfkdildkielignenhglyladqyvkgiaksrks*

Antigen expression and purification from stable CHO manufacturing cell line

DNA for RSV pre-F-NP constructs was synthesized and cloned into an in-house mammalian expression vector. Each resulting RSV pre-F-NP expression vector was transfected into in-house CHO cells by electroporation, followed by methotrexate selection to isolate stably transfected cell pools. CHO cell clones expressing RSV pre-F-NP RF8140 were isolated from a pool by flow cytometric sorting and deposition into 96-well plates at one cell per well. To generate RSV pre-F-NP material from CHO pools and clones, cells were seeded into CD CHO medium (Thermo Fisher Scientific) supplemented with 30% (v/v) EfficientFeed B (Thermo Fisher Scientific) and 4 mM L-glutamine and incubated in suspension culture for 7 days. Conditioned media harvests were clarified and used for analysis of RSV pre-F-NP titer.

Sc-pre-F-NP was initially tested in stably transfected CHO cell pools, expressing at a low yield (~10 mg/liter from stable pools) and exhibiting nonspecific proteolytic cleavage between the F and ferritin moieties. Mutations to potentially susceptible residues in the F stalk and a bullfrog ferritin-linker region were introduced resulting in pre-F-NP for CHO cell line development. Pre-F-NP in stable CHO cell pools expressed up to 89 mg/liter as measured by AM14-binding using Octet (below). Final CHO clones express between ~150 and 300 mg/liter. Material used for the mouse dosing study was purified from stable CHO clone using similar anion exchange methods as above but without size exclusion purification.

RSV F nanoparticle sequence for CHO manufacturability

Pre-F-NP. mellilkanaittiltavtfcfasgqniteefyqstcsavskgylsalrtgwytsvitielsnikenkcngtdakvklikqeldkyknavtelqllmgsgnvglggaiasgvavskvlhlegevnkiksallstnkavvslsngvsvltfkvldlknyidkqllpilnkqscsisnpetviefqqknnrlleitrefsvnagvttpvstymltnsellslindmpitndqkklmsnnvqivrqqsysimsiikeevlayvvqlplygvidtpcwklhtsplcttntkngsnicltrtdrgwycdnagnvsffpqaetckvqsnrvfcdtmnsrtlpsevnlcnvdifnpkydckimtsktdvsssvitslgaivscygktkctasnknrgiiktfsngcdyvsnkgvdtvsvgntlyyvnkqegkslyvkgepiinfydplvfpsdefdasisqvnelinqslafinqsdellsgsgsesqvqqqfskdiekllneqvnkemqssnlymsmsswsythsldgaglflfdhaaeeyehakkliiflnennvpvqltsisapehcfegltqifqkayeheqhisesinnivdhaikskdhatfnflqwyvaeqheeevlfkdildkielignenhglyladqyvkgiaksrks*

F nanoparticle expression by AM14-binding using Octet

The expression yields of pre-F antigens were measured using pre-F–specific Ab AM14 using a FortéBio Octet RED96 instrument. All assays were performed with binding buffer [phosphate-buffered saline (PBS) supplemented with 2% bovine serum albumin (BSA)] to minimize nonspecific interactions at 30°C. AM14 was loaded onto Protein A sensor tips (FortéBio) for 300 s to allow capture to approach saturation. Biosensor tips were then equilibrated for 30 s in binding buffer before measurement of association with pre-F-NP standards or conditioned media from nanoparticle expression diluted 1:1 in binding buffer for 200 s. Tips were regenerated between measurements using glycine (pH 1.5) (GE Healthcare). Sample concentrations were determined by comparing initial 50-s association rates, after applying dilution factor, with a linear standard curve generated from the pre-F-NP standards using the Octet Data Analysis software, version 10.0.

NAb-binding by SPR (Biacore)

The affinities of pre-F-NP and pre-F for NAbs (palivizumab, 101F, D25, and AM14) were measured by surface plasmon resonance (SPR) with a Biacore T200 instrument. Abs were directly immobilized on a protein A sensor chip (GE Healthcare) at low levels (~2 to 10 response units), and antigens at various concentrations were injected at a high flow rate (50 μl/min) to avoid avidity effects. The data were processed using Biacore T200 evaluation software and double-referenced by subtraction of the blank surface and buffer-only injection values before global fitting of the data to a 1:1 binding model.

Evaluation of nanoparticles by negative-staining EM

EM was performed by NanoImaging Services (San Diego, CA). Sc-pre-F-NP was diluted into PBS to about 20 μg/ml and imaged over a layer of continuous carbon supported by nitrocellulose on a 400-mesh copper grid. The sample was prepared by applying 3-μl sample suspension to a freshly plasma cleaned grid, blotting away with filter paper, and immediately staining with 3 μl of 2% uranyl formate. EM was performed using an FEI Tecnai T12 electron microscope operating at 120 keV and equipped with an FEI Eagle 4k × 4k charge-coupled device camera. Images were obtained using Leginon at a nominal magnification of ×67,000 (0.16 nm/pixel), nominal under focus of −0.8 to −1.5 μm, and electron dose of −30 $e^{-}/Å^{2}$ (*50*). Image processing was performed using the Appion software package (*51*). The contrast transfer functions of the images were estimated and corrected using CTFFIND4 (*52*). Individual particles in the images were selected using automated picking protocols and submitted to several rounds of reference-free alignment and classification using the XMIPP package (*53*, *54*).

Mouse immunizations

In initial screening studies, female BALB/c mice were intramuscularly immunized with RSV antigens (prepared from transient transfection) at 0.1-μg doses at weeks 0, 3, and 6. Each group contained five mice. Antigens were prepared by mixing 50-μl protein solution with 50 μl of AF03 just before immunization of 50 μl into each hind leg. Blood was collected 1 day before first immunization (for control samples) and 2 weeks after immunogen injection (i.e., weeks 5 and 8).

For mouse dosing study (Fig. 5 and fig. S3), CHO-derived pre-F-NP was used. Antigens were prepared by mixing 25-μl protein solution with an equal volume of PBS or AF03. Groups of eight female BALB/c mice were intramuscularly immunized in one leg with 50-μl antigen with or without AF03. Groups were dosed at 0.03, 0.1, 0.3, 1, 3, 9, or 27 μg as indicated. Blood was collected at day 21 (week 3) and day 35 (week 5) for analysis.

NHP immunizations

Cynomolgus macaques were housed at Cynbiose SA (Marcy l'Etoile, France). This study was reviewed by the Animal Welfare Body of Cynbiose and the Ethics Committee of VetAgro Sup (1 avenue Bourgelat, 69280 Marcy l'Étoile, France) and approved under number 1633-V3 (MESR number: 2016071517212815). All experiments were conducted in accordance with the European Directive 2010/63/UE as published in the French Official Journal of 7 February 2013.

Eight RSV-seronegative adult cynomolgus macaques (24 to 30 months old) were randomized into two immunization groups of four animals each. Fifty micrograms of pre-F-NP with PBS (nonadjuvanted) or pre-F-NP with AF03 was administered intramuscularly into the deltoid muscle at days 0 and 28. Sera were collected before immunization and at different time points after immunization.

Mouse sera pre-F– and post-F–binding Ab titer ELISA using Octet

Heat-inactivated sera from mice immunized with antigens were diluted in PBS with 2% BSA. Sera from week 5 were diluted 1:100 and sera from week 8 were diluted 1:300 to prevent saturation of the association curve. RSV F trimers (pre-F or post-F) were loaded onto anti–penta-HIS (HIS1K) sensor tips (FortéBio) for 400 s to allow capture to reach near saturation. Biosensor tips were then equilibrated for 90 s in Octet Wash Buffer, followed by diluted sera association for 300 s. Association curve final responses were measured using Octet Data Analysis HT10.0 software, and the response was multiplied by the dilution factor to obtain the final reported response.

NHP sera F-binding Ab titer ELISA

RSV-F–specific Ab titers were tested by ELISA. Briefly, microtiter plates (Dynex, Nunc) were coated with either pre-F or post-F protein

(1 μg/ml) (Sino Biological) in bicarbonate buffer (Sigma-Aldrich). Plates were incubated overnight at 4°C and then blocked with PBS–0.05% Tween–5% milk for 1 hour. Sera were serially diluted in PBS–0.05% Tween–5% milk in the coated plate. After 1.5 hours of incubation at 37°C, plates were washed (PBS–0.05% Tween) and incubated for 1.5 hours at 37°C with a goat anti-monkey IgG–horseradish peroxidase (HRP) diluted at 1:10,000 (Bio-Rad). After washing, plates were incubated with tetramethylbenzidine substrate (tebu-bio) for 30 min in the dark at room temperature. Colorimetric reaction was stopped with 100 μl per well of 1 M HCl (VWR Prolabo). Optical density (OD) was measured at 450 and 650 nm on a VersaMax plate reader (Molecular Devices).

D25 competitive ELISA

DS-Cav1 was coated on microtiter plates (Greiner Bio-One) overnight at 4°C and then blocked with PBS–0.05% Tween–5% nonfat dry milk for 1 hour at 37°C. Sera were serially diluted twofold (initial dilution, 1:5) and incubated for 1.5 hours at 37°C. After PBS–0.05% Tween washes, competitive biotinylated D25 Ab was added and incubated for 30 min at 37°C. Plates were washed and an anti-biotin HRP conjugate (Invitrogen) was added for 1.5 hours at 37°C. After washing, the plates were developed using 3,3,5,5-tetramethylbenzidine (tebu-bio) and stopped with 1 M HCl (Prolabo). ODs were read at 450 to 650 nm. After blank subtraction, the percentage of inhibition was calculated as follows: [1 − (sera OD)/(baseline OD)] × 100. The dilution needed to achieve 50% of inhibition was obtained by a four-parameter logistic regression.

NAb titer analysis for mouse and NHP studies

Mouse and NHP 60% plaque reduction neutralization titers ($PRNT_{60}$) were determined by a method similar to that previously described without complement (*55*). Briefly, RSV viral stocks were combined 1:1 with dilutions of heat-inactivated serum and incubated for 1 to 1.5 hours at 37°C. The virus-serum mixture was centrifuged and added to plates containing confluent Vero cell monolayers and incubated for 1 to 1.5 hours at 37°C. After incubation at 37°C, the overlay was removed and the monolayers were fixed and stained with labeled anti-RSV Ab and stained. The stained plaques were counted using a dissecting microscope, and the NAb titers were determined at the 60% reduction endpoint.

MIMIC analysis

Apheresis blood products were collected from 48 healthy human donors. The collections and study protocol were reviewed and approved by Chesapeake Research Review Inc. under IRB 0906009. Donor plasma and peripheral blood mononuclear cells were cryopreserved and stored for an extended period of time in vapor-phase nitrogen tanks.

To evaluate humoral responses to RSV and F candidates, differentiated donor antigen-presenting cells were stimulated with no antigen live RSV [multiplicity of infection (MOI), 0.005] and F antigens (pre-F-NP, post-F, and pre-F at 10 ng/ml) as previously described (*40*). $CD19^+$ B cells were enriched and cultured with F antigens or left untreated. After priming with antigens, antigen-presenting cells were cocultured with enriched autologous $CD4^+$ T cells and pretreated $CD19^+$ B cells for 14 days and culture supernatants were collected for detection of anti-RSV, anti–pre-F, or anti–post-F IgG Abs. Detailed intracellular cytokine staining protocols were described elsewhere (*40*, *56*).

Antibody Forensics

Culture supernatants from MIMIC studies were collected for detection of RSV antigen-specific IgG by a multiplexed Luminex-based method called "Antibody Forensics" previously described in detail (*40*). Briefly, fluorescent carboxylated magnetic beads (Luminex) were activated and coated directly with RSV proteins (20 μg/ml) (pre-F or post-F) to detect protein-specific IgG (*40*). The antigen-loaded Luminex beads incubated with MIMIC supernatants or plasma from patient samples were analyzed on the Bio-Plex 100 System (Bio-Rad).

Microneutralization assay for MIMIC system

The neutralization activity of supernatants from MIMIC cultures was measured using Vero cells infected with a subtype A mKate-expressing RSV (RSV A2-mKate). RSV A2-mKate at MOI 0.15 was added to serial twofold dilutions (beginning with a dilution of 1:2) of MIMIC supernatant, or BEI reference sera NR-4022 (beginning at a dilution of 1:20) were incubated at 37°C for 1 hour. Then, the mixture was added to infect 25,000 Vero cells. Fluorescent cell counting of RSV-mKate–infected Vero cells was performed using a Celigo microplate reader with an excitation wavelength of 531 nm and an emission wavelength of 629 nm (Celigo, Nexcelom Bioscience) after 24 hours of incubation. Neutralizing titer was calculated for the 50% reduction of viral infection and was converted to international units per milliliter using the NR-4022 reference control serum for RSV, following the World Health Organization instructions (*57*).

Statistics

Statistics were computed with Prism version 6.0 (GraphPad), SAS version 13, and JMP Pro 13. For mouse and NHP studies, the *P* values were derived by Student's *t* test. For MIMIC studies, the geometric mean of the pairwise differences between Ab titers in groups after treatment was analyzed using Tukey's post hoc test with SAS software version 9.4. The difference of geometric means of Ab titers between age groups was compared using a two-tailed unpaired *t* test.

SUPPLEMENTARY MATERIALS

immunology.sciencemag.org/cgi/content/full/5/47/eaba6466/DC1

Fig. S1. Durability of pre-F response elicited in NHP immunized with pre-F-NP and AF03 adjuvant.

Fig. S2. Homogeneity and antigenicity of CHO-derived pre-F-NP.

Fig. S3. NAb responses to pre-F and pre-F-NP in mice is dependent on immunogen dose.

Fig. S4. Representation of pre-F–binding titers stimulated by RSV antigens for all individuals tested in the MIMIC system.

Fig. S5. Similar RSV-specific Ab and $CD4^+$ T cell responses are elicited in adult and elderly donors after in vitro vaccination in the MIMIC system.

Table S1. Raw data file (Excel spreadsheet).

View/request a protocol for this paper from *Bio-protocol*.

REFERENCES AND NOTES

1. A. D. Colosia, J. Yang, E. Hillson, J. Mauskopf, C. Copley-Merriman, V. Shinde, J. Stoddard, The epidemiology of medically attended respiratory syncytial virus in older adults in the United States: A systematic review. *PLOS ONE* **12**, e0182321 (2017).
2. S. Nye, R. J. Whitley, M. Kong, Viral infection in the development and progression of pediatric acute respiratory distress syndrome. *Front. Pediatr.* **4**, 128 (2016).
3. K. Haq, J. E. McElhaney, Immunosenescence: Influenza vaccination and the elderly. *Curr. Opin. Immunol.* **29**, 38–42 (2014).
4. J. E. McElhaney, G. A. Kuchel, X. Zhou, S. L. Swain, L. Haynes, T-cell immunity to influenza in older adults: A pathophysiological framework for development of more effective vaccines. *Front. Immunol.* **7**, 41 (2016).
5. A. Pera, C. Campos, N. López, F. Hassouneh, C. Alonso, R. Tarazona, R. Solana, Immunosenescence: Implications for response to infection and vaccination in older people. *Maturitas* **82**, 50–55 (2015).

6. A. Cherukuri, K. Patton, R. A. Gasser Jr., F. Zuo, J. Woo, M. T. Esser, R. S. Tang, Adults 65 years old and older have reduced numbers of functional memory T cells to respiratory syncytial virus fusion protein. *Clin. Vaccine Immunol.* **20**, 239–247 (2013).
7. P. L. Acosta, M. T. Caballero, F. P. Polack, Brief history and characterization of enhanced respiratory syncytial virus disease. *Clin. Vaccine Immunol.* **23**, 189–195 (2015).
8. N. I. Mazur, D. Higgins, M. C. Nunes, J. A. Melero, A. C. Langedijk, N. Horsley, U. J. Buchholz, P. J. Openshaw, J. McLellan, J. A. Englund, A. Mejias, R. A. Karron, E. A. F. Simões, I. Knezevic, O. Ramilo, P. A. Piedra, H. Y. Chu, A. R. Falsey, H. Nair, L. Kragten-Tabatabaie, A. Greenough, E. Baraldi, N. G. Papadopoulos, J. Vekemans, F. P. Polack, M. Powell, A. Satav, E. E. Walsh, R. T. Stein, B. S. Graham, L. J. Bont; Respiratory Syncytial Virus Network (ReSViNET) Foundation, The respiratory syncytial virus vaccine landscape: Lessons from the graveyard and promising candidates. *Lancet Infect. Dis.* **18**, e295–e311 (2018).
9. A. Noor, L. R. Krilov, Respiratory syncytial virus vaccine: Where are we now and what comes next? *Expert Opin. Biol. Ther.* **18**, 1247–1256 (2018).
10. B. S. Graham, Vaccine development for respiratory syncytial virus. *Curr. Opin. Virol.* **23**, 107–112 (2017).
11. B. S. Graham, K. Modjarrad, J. S. McLellan, Novel antigens for RSV vaccines. *Curr. Opin. Immunol.* **35**, 30–38 (2015).
12. N. Jaberolansar, I. Toth, P. R. Young, M. Skwarczynski, Recent advances in the development of subunit-based RSV vaccines. *Expert Rev. Vaccines* **15**, 53–68 (2016).
13. European Medicines Agency, Recombinant respiratory syncytial virus vaccine—Notification of discontinuation of a paediatric development which is covered by an agreed PIP Decision (MEDI7510, EMA document, 2016) [cited 16 January 2018], pp. 1–2; http://www.ema.europa.eu/docs/en_GB/document_library/Other/2016/11/WC500216809.pdf.
14. Globe Newswire, Novavax announces topline RSV F vaccine data from two clinical trials in older adults. Novavax press release (2016) [cited 16 January 2018], pp. 1–2; https://ir.novavax.com/news-releases/news-release-details/novavax-announces-topline-rsv-f-vaccine-data-two-clinical-trials.
15. G. Bolt, L. Ø. Pedersen, H. H. Birkeslund, Cleavage of the respiratory syncytial virus fusion protein is required for its surface expression: Role of furin. *Virus Res.* **68**, 25–33 (2000).
16. L. González-Reyes, M. B. Ruiz-Argüello, B. García-Barreno, L. Calder, J. A. López, J. P. Albar, J. J. Skehel, D. C. Wiley, J. A. Melero, Cleavage of the human respiratory syncytial virus fusion protein at two distinct sites is required for activation of membrane fusion. *Proc. Natl. Acad. Sci. U.S.A.* **98**, 9859–9864 (2001).
17. J. S. McLellan, M. Chen, S. Leung, K. W. Graepel, X. Du, Y. Yang, T. Zhou, U. Baxa, E. Yasuda, T. Beaumont, A. Kumar, K. Modjarrad, Z. Zheng, M. Zhao, N. Xia, P. D. Kwong, B. S. Graham, Structure of RSV fusion glycoprotein trimer bound to a prefusion-specific neutralizing antibody. *Science* **340**, 1113–1117 (2013).
18. J. S. McLellan, Y. Yang, B. S. Graham, P. D. Kwong, Structure of respiratory syncytial virus fusion glycoprotein in the postfusion conformation reveals preservation of neutralizing epitopes. *J. Virol.* **85**, 7788–7796 (2011).
19. K. A. Swanson, E. C. Settembre, C. A. Shaw, A. K. Dey, R. Rappuoli, C. W. Mandl, P. R. Dormitzer, A. Carfi, Structural basis for immunization with postfusion respiratory syncytial virus fusion F glycoprotein (RSV F) to elicit high neutralizing antibody titers. *Proc. Natl. Acad. Sci. U.S.A.* **108**, 9619–9624 (2011).
20. A. Krarup, D. Truan, P. Furmanova-Hollenstein, L. Bogaert, P. Bouchier, I. J. M. Bisschop, M. N. Widjojoatmodjo, R. Zahn, H. Schuitemaker, J. S. McLellan, J. P. M. Langedijk, A highly stable prefusion RSV F vaccine derived from structural analysis of the fusion mechanism. *Nat. Commun.* **6**, 8143 (2015).
21. J. S. McLellan, M. Chen, M. G. Joyce, M. Sastry, G. B. E. Stewart-Jones, Y. Yang, B. Zhang, L. Chen, S. Srivatsan, A. Zheng, T. Zhou, K. W. Graepel, A. Kumar, S. Moin, J. C. Boyington, G.-Y. Chuang, C. Soto, U. Baxa, A. Q. Bakker, H. Spits, T. Beaumont, Z. Zheng, N. Xia, S.-Y. Ko, J.-P. Todd, S. Rao, B. S. Graham, P. D. Kwong, Structure-based design of a fusion glycoprotein vaccine for respiratory syncytial virus. *Science* **342**, 592–598 (2013).
22. M. G. Joyce, B. Zhang, L. Ou, M. Chen, G.-Y. Chuang, A. Druz, W.-P. Kong, Y.-T. Lai, E. J. Rundlet, Y. Tsybovsky, Y. Yang, I. S. Georgiev, M. Guttman, C. R. Lees, M. Pancera, M. Sastry, C. Soto, G. B. E. Stewart-Jones, P. V. Thomas, J. G. van Galen, U. Baxa, K. K. Lee, J. R. Mascola, B. S. Graham, P. D. Kwong, Iterative structure-based improvement of a fusion-glycoprotein vaccine against RSV. *Nat. Struct. Mol. Biol.* **23**, 811–820 (2016).
23. M. C. Crank, T. J. Ruckwardt, M. Chen, K. M. Morabito, E. Phung, P. J. Costner, L. A. Holman, S. P. Hickman, N. M. Berkowitz, I. J. Gordon, G. V. Yamshchikov, M. R. Gaudinski, A. Kumar, L. A. Chang, S. M. Moin, J. P. Hill, A. T. DiPiazza, R. M. Schwartz, L. Kueltzo, J. W. Cooper, P. Chen, J. A. Stein, K. Carlton, J. G. Gall, M. C. Nason, P. D. Kwong, G. L. Chen, J. R. Mascola, J. S. McLellan, J. E. Ledgerwood, B. S. Graham; VRC 317 Study Team, A proof of concept for structure-based vaccine design targeting RSV in humans. *Science* **365**, 505–509 (2019).
24. J. S. McLellan, W. C. Ray, M. E. Peeples, Structure and function of respiratory syncytial virus surface glycoproteins. *Curr. Top. Microbiol. Immunol.* **372**, 83–104 (2013).
25. K. Vaughan, J. Ponomarenko, B. Peters, A. Sette, Analysis of human RSV immunity at the molecular level: Learning from the past and present. *PLOS ONE* **10**, e0127108 (2015).
26. K. A. Swanson, K. Balabanis, Y. Xie, Y. Aggarwal, C. Palomo, V. Mas, C. Metrick, H. Yang, C. A. Shaw, J. A. Melero, P. R. Dormitzer, A. Carfi, A monomeric uncleaved respiratory syncytial virus F antigen retains prefusion-specific neutralizing epitopes. *J. Virol.* **88**, 11802–11810 (2014).
27. J. Marcandalli, B. Fiala, S. Ols, M. Perotti, W. de van der Schueren, J. Snijder, E. Hodge, M. Benhaim, R. Ravichandran, L. Carter, W. Sheffler, L. Brunner, M. Lawrenz, P. Dubois, A. Lanzavecchia, F. Sallusto, K. K. Lee, D. Veesler, C. E. Correnti, L. J. Stewart, D. Baker, K. Loré, L. Perez, N. P. King, Induction of potent neutralizing antibody responses by a designed protein nanoparticle vaccine for respiratory syncytial virus. *Cell* **176**, 1420–1431.e17 (2019).
28. C. Osiowy, D. Horne, R. Anderson, Antibody-dependent enhancement of respiratory syncytial virus infection by sera from young infants. *Clin. Diagn. Lab. Immunol.* **1**, 670–677 (1994).
29. L. R. Krilov, L. J. Anderson, L. Marcoux, V. R. Bonagura, J. F. Wedgwood, Antibody-mediated enhancement of respiratory syncytial virus infection in two monocyte/macrophage cell lines. *J. Infect. Dis.* **160**, 777–782 (1989).
30. E. A. van Erp, P. B. van Kasteren, T. Guichelaar, I. M. L. Ahout, C. A. M. de Haan, W. Luytjes, G. Ferwerda, O. Wicht, In vitro enhancement of respiratory syncytial virus infection by maternal antibodies does not explain disease severity in infants. *J. Virol.* **91**, e00851-17 (2017).
31. M. Kanekiyo, M. G. Joyce, R. A. Gillespie, J. R. Gallagher, S. F. Andrews, H. M. Yassine, A. K. Wheatley, B. E. Fisher, D. R. Ambrozak, A. Creanga, K. Leung, E. S. Yang, S. Boyoglu-Barnum, I. S. Georgiev, Y. Tsybovsky, M. S. Prabhakaran, H. Andersen, W.-P. Kong, U. Baxa, K. L. Zephir, J. E. Ledgerwood, R. A. Koup, P. D. Kwong, A. K. Harris, A. B. McDermott, J. R. Mascola, B. S. Graham, Mosaic nanoparticle display of diverse influenza virus hemagglutinins elicits broad B cell responses. *Nat. Immunol.* **20**, 765 (2019).
32. M. Kanekiyo, C.-J. Wei, H. M. Yassine, P. M. McTamney, J. C. Boyington, J. R. R. Whittle, S. S. Rao, W.-P. Kong, L. Wang, G. J. Nabel, Self-assembling influenza nanoparticle vaccines elicit broadly neutralizing H1N1 antibodies. *Nature* **499**, 102–106 (2013).
33. H. M. Yassine, J. C. Boyington, P. M. McTamney, C.-J. Wei, M. Kanekiyo, W.-P. Kong, J. R. Gallagher, L. Wang, Y. Zhang, M. G. Joyce, D. Lingwood, S. M. Moin, H. Andersen, Y. Okuno, S. S. Rao, A. K. Harris, P. D. Kwong, J. R. Mascola, G. J. Nabel, B. S. Graham, Hemagglutinin-stem nanoparticles generate heterosubtypic influenza protection. *Nat. Med.* **21**, 1065–1070 (2015).
34. N. Darricarrère, S. Pougatcheva, X. Duan, R. S. Rudicell, T.-H. Chou, J. D. Napoli, T. M. Ross, T. Alefantis, T. U. Vogel, H. Kleanthous, C.-J. Wei, G. J. Nabel, Development of a Pan-H1 influenza vaccine. *J. Virol.* **92**, e01349-18 (2018).
35. M. Kanekiyo, W. Bu, M. G. Joyce, G. Meng, J. R. R. Whittle, U. Baxa, T. Yamamoto, S. Narpala, J.-P. Todd, S. S. Rao, A. B. McDermott, R. A. Koup, M. G. Rossmann, J. R. Mascola, B. S. Graham, J. I. Cohen, G. J. Nabel, Rational design of an Epstein-Barr virus vaccine targeting the receptor-binding site. *Cell* **162**, 1090–1100 (2015).
36. D. Drake III, I. Singh, M. N. Nguyen, A. Kachurin, V. Wittman, R. Parkhill, O. Kachurina, J. M. Moser, N. Burdin, M. Moreau, N. Mistretta, A. M. Byers, V. Dhir, T. M. Tapia, C. Vernhes, J. Gangur, T. Kamala, N. Swaminathan, W. L. Warren, In vitro biomimetic model of the human immune system for predictive vaccine assessments. *Disrupt. Sci. Technol.* **1**, 28–40 (2012).
37. I. Yamashita, K. Iwahori, S. Kumagai, Ferritin in the field of nanodevices. *Biochim. Biophys. Acta* **1800**, 846–857 (2010).
38. M. S. A. Gilman, S. M. Moin, V. Mas, M. Chen, N. K. Patel, K. Kramer, Q. Zhu, S. C. Kabeche, A. Kumar, C. Palomo, T. Beaumont, U. Baxa, N. D. Ulbrandt, J. A. Melero, B. S. Graham, J. S. McLellan, Characterization of a prefusion-specific antibody that recognizes a quaternary, cleavage-dependent epitope on the RSV fusion glycoprotein. *PLOS Pathog.* **11**, e1005035 (2015).
39. M.-F. Klucker, F. Dalencon, P. Probeck, J. Haensler, AF03, an alternative squalene emulsion-based vaccine adjuvant prepared by a phase inversion temperature method. *J. Pharm. Sci.* **101**, 4490–4500 (2012).
40. A. Dauner, P. Agrawal, J. Salvatico, T. Tapia, V. Dhir, S. F. Shaik, D. R. Drake III, A. M. Byers, The in vitro MIMIC® platform reflects age-associated changes in immunological responses after influenza vaccination. *Vaccine* **35**, 5487–5494 (2017).
41. A. M. Byers, T. M. Tapia, E. R. Sassano, V. Wittman, In vitro antibody response to tetanus in the MIMIC™ system is a representative measure of vaccine immunogenicity. *Biologicals* **37**, 148–151 (2009).
42. R. G. Higbee, A. M. Byers, V. Dhir, D. Drake, H. G. Fahlenkamp, J. Gangur, A. Kachurin, O. Kachurina, D. Leistritz, Y. Ma, R. Mehta, E. Mishkin, J. Moser, L. Mosquera, M. Nguyen, R. Parkhill, S. Pawar, L. Poisson, G. Sanchez-Schmitz, B. Schanen, I. Singh, H. Song, T. Tapia, W. Warren, V. Wittman, An immunologic model for rapid vaccine assessment—A clinical trial in a test tube. *Altern. Lab. Anim.* **37** (suppl. 1), 19–27 (2009).
43. D. K. Edwards, E. Jasny, H. Yoon, N. Horscroft, B. Schanen, T. Geter, M. Fotin-Mleczek, B. Petsch, V. Wittman, Adjuvant effects of a sequence-engineered mRNA vaccine: Translational profiling demonstrates similar human and murine innate response. *J. Transl. Med.* **15**, 1 (2017).

44. B. Bagga, J. E. Cehelsky, A. Vaishnaw, T. Wilkinson, R. Meyers, L. M. Harrison, P. L. Roddam, E. E. Walsh, J. P. DeVincenzo, Effect of preexisting serum and mucosal antibody on experimental respiratory syncytial virus (RSV) challenge and infection of adults. *J. Infect. Dis.* **212**, 1719–1725 (2015).
45. O. T. Idoko, S. N. Okolo, B. Plikaytis, A. Akinsola, S. Viviani, R. Borrow, G. Carlone, H. Findlow, C. Elie, P. S. Kulkarni, M.-P. Preziosi, M. Ota, B. Kampmann, The impact of pre-existing antibody on subsequent immune responses to meningococcal A-containing vaccines. *Vaccine* **32**, 4220–4227 (2014).
46. B. R. Murphy, D. W. Alling, M. H. Snyder, E. E. Walsh, G. A. Prince, R. M. Chanock, V. G. Hemming, W. J. Rodriguez, H. W. Kim, B. S. Graham, Effect of age and preexisting antibody on serum antibody response of infants and children to the F and G glycoproteins during respiratory syncytial virus infection. *J. Clin. Microbiol.* **24**, 894–898 (1986).
47. A. R. Falsey, E. E. Walsh, Relationship of serum antibody to risk of respiratory syncytial virus infection in elderly adults. *J. Infect. Dis.* **177**, 463–466 (1998).
48. C. Terrosi, G. Di Genova, B. Martorelli, M. Valentini, M. G. Cusi, Humoral immunity to respiratory syncytial virus in young and elderly adults. *Epidemiol. Infect.* **137**, 1684–1686 (2009).
49. J. S. McLellan, M. Chen, A. Kim, Y. Yang, B. S. Graham, P. D. Kwong, Structural basis of respiratory syncytial virus neutralization by motavizumab. *Nat. Struct. Mol. Biol.* **17**, 248–250 (2010).
50. C. Suloway, J. Pulokas, D. Fellmann, A. Cheng, F. Guerra, J. Quispe, S. Stagg, C. S. Potter, B. Carragher, Automated molecular microscopy: The new Leginon system. *J. Struct. Biol.* **151**, 41–60 (2005).
51. N. R. Voss, D. Lyumkis, A. Cheng, P.-W. Lau, A. Mulder, G. C. Lander, E. J. Brignole, D. Fellmann, C. Irving, E. L. Jacovetty, A. Leung, J. Pulokas, J. D. Quispe, H. Winkler, C. Yoshioka, B. Carragher, C. S. Potter, A toolbox for ab initio 3-D reconstructions in single-particle electron microscopy. *J. Struct. Biol.* **169**, 389–398 (2010).
52. A. Rohou, N. Grigorieff, CTFFIND4: Fast and accurate defocus estimation from electron micrographs. *J. Struct. Biol.* **192**, 216–221 (2015).
53. N. R. Voss, C. K. Yoshioka, M. Radermacher, C. S. Potter, B. Carragher, DoG Picker and TiltPicker: Software tools to facilitate particle selection in single particle electron microscopy. *J. Struct. Biol.* **166**, 205–213 (2009).
54. C. O. S. Sorzano, R. Marabini, J. Velázquez-Muriel, J. R. Bilbao-Castro, S. H. W. Scheres, J. M. Carazo, A. Pascual-Montano, XMIPP: A new generation of an open-source image processing package for electron microscopy. *J. Struct. Biol.* **148**, 194–204 (2004).
55. R. Groppo, J. DiNapoli, K. Il Jeong, M. Kishko, N. Jackson, H. Kleanthous, S. Delagrave, L. Zhang, M. Parrington, Effect of genetic background and delivery route on the preclinical properties of a live attenuated RSV vaccine. *PLOS ONE* **13**, e0199452 (2018).
56. B. C. Schanen, A. S. De Groot, L. Moise, M. Ardito, E. McClaine, W. Martin, V. Wittman, W. L. Warren, D. R. Drake III, Coupling sensitive in vitro and in silico techniques to assess cross-reactive $CD4^+$ T cells against the swine-origin H1N1 influenza virus. *Vaccine* **29**, 3299–3309 (2011).
57. J. U. McDonald, P. Rigsby, T. Dougall, O. G. Engelhardt; Study Participants, Establishment of the first WHO International Standard for antiserum to Respiratory Syncytial Virus: Report of an international collaborative study. *Vaccine* **36**, 7641–7649 (2018).

Acknowledgments: We thank Y. Lewis for protein expression and purification support. We thank R. Bodinizzo, K. Balko, E. Hunter, M. Pike, H. Bisceglia, S. Montano, and F. Guillaume for their contributions to the animal experiments and analytical assays. We thank P. Jurvilliers and I. Ordonez for assistance with statistical analysis. We thank J. Moser for support with the MIMIC studies. We thank J. Zhang, C. DeMaria, and J. Ni for CHO cell line generation and purification support. We thank J. Ackroyd, a medical writer at InScience Communications, for editorial assistance. We thank A.E. Schroeer and B. DelGiudice for assistance in figure preparations. **Funding:** This work was supported by Sanofi R&D. **Author contributions:** K.A.S., J.N.R.-T., Z.P.W., V.P., L.Z., N.J., C.-J.W., and G.J.N. designed research studies. K.A.S., J.N.R.-T., Z.P.W., L.L., M.P., M.K., J.A.-S., H.A., S. Gupta, S.C., H.Y., and D.E. performed the research, K.A.S., J.N.R.-T., Z.P.W., L.L., M.P., M.K., V.P., J.A.-S., H.A., S. Gupta, S.C., S. Gallichan, L.Z., N.J., H.Y., D.E., C.-J.W., and G.J.N. interpreted and discussed the data. K.A.S., J.N.R.-T., Z.P.W., C.-J.W., and G.J.N. wrote the paper, and all authors participated in manuscript revisions. **Competing interests:** At the time the research described in this manuscript was performed, K.A.S., J.N.R.-T., Z.P.W., L.L., M.P., M.K., V.P., J.A.-S., H.A., S. Gupta, S.C., S. Gallichan, L.Z., N.J., H.Y., D.E., C.-J.W., and G.J.N. were employees of Sanofi and/or its subsidiary Sanofi-Pasteur, which has filed patent applications on RSV vaccines. K.A.S., C.-J.W., and G.J.N. are inventors on the international patent application PCT/US2019/025387 titled "Antigenic respiratory syncytial virus polypeptides." **Data and materials availability:** The materials that support the findings of this study are available from the corresponding author upon request. All data needed to evaluate the conclusions in the paper are present in the paper or the Supplementary Materials.

Submitted 19 December 2019
Accepted 9 April 2020
Published 1 May 2020
10.1126/sciimmunol.aba6466

Citation: K. A. Swanson, J. N. Rainho-Tomko, Z. P. Williams, L. Lanza, M. Peredelchuk, M. Kishko, V. Pavot, J. Alamares-Sapuay, H. Adhikarla, S. Gupta, S. Chivukula, S. Gallichan, L. Zhang, N. Jackson, H. Yoon, D. Edwards, C.-J. Wei, G. J. Nabel, A respiratory syncytial virus (RSV) F protein nanoparticle vaccine focuses antibody responses to a conserved neutralization domain. *Sci. Immunol.* **5**, eaba6466 (2020).

Science Immunology

A respiratory syncytial virus (RSV) F protein nanoparticle vaccine focuses antibody responses to a conserved neutralization domain

Kurt A. Swanson, Jennifer N. Rainho-Tomko, Zachary P. Williams, Lilibeth Lanza, Michael Peredelchuk, Michael Kishko, Vincent Pavot, Judith Alamares-Sapuay, Haritha Adhikarla, Sankalp Gupta, Sudha Chivukula, Scott Gallichan, Linong Zhang, Nicholas Jackson, Heesik Yoon, Darin Edwards, Chih-Jen Wei and Gary J. Nabel

Sci. Immunol. **5**, eaba6466.
DOI: 10.1126/sciimmunol.aba6466

Sharpening the focus of anti-RSV antibodies

Respiratory syncytial virus (RSV) is a paramyxovirus that infects lung epithelial cells causing potentially severe infections in young children, the elderly, and the immunocompromised. Although an effective RSV vaccine remains a major unmet medical need, previous work has identified a stabilized pre-F conformation of the RSV fusion (F) protein as a preferred immunogen for eliciting neutralizing antibodies. Swanson *et al*. constructed a multimeric vaccine featuring a central ferritin core connected to eight trimeric pre-F spikes bearing engineered glycans that mask poorly neutralizing epitopes. This self-assembling nanoparticle vaccine induced stronger neutralizing antibody responses than pre-F trimers in both mice and nonhuman primates. These studies pave the way toward initiating clinical trials to test this vaccine's ability to protect vulnerable human populations from RSV-associated disease.